Exergy Balance Decomposition Between Mechanically-and Thermally-Recoverable Exergy Ouflows

Ilyès Berhouni, Didier Bailly, Ilias Petropoulos

Exergy Balance Decomposition Between Mechanically- and Thermally-Recoverable Exergy Ouflows

Ilyès Berhouni*, Didier Bailly†, Ilias Petropoulos‡
ONERA - The French Aerospace Lab, Meudon, F-92190, France

Nomenclature

$\dot{A}^o$	=	Outflow rate of anergy through S_o, J.s^{-1}
$\dot{\mathcal{A}}_w$	=	Rate of anergy generation by shockwaves, J.s^{-1}
$\dot{\mathcal{A}}_{\nabla T}$	=	Rate of anergy generation by thermal mixing, J.s^{-1}
$\dot{\mathcal{A}}_\phi$	=	Rate of anergy generation by viscous dissipation, J.s^{-1}
c_p	=	Specific heat capacity at constant pressure, J.K^{-1}.kg^{-1}
$\dot{E}^o_u$	=	Streamwise kinetic energy outflow, J.s^{-1}
$\dot{E}^o_{vw}$	=	Transverse kinetic energy outflow, J.s^{-1}
$\dot{E}^o_p$	=	Boundary pressure-work rate, J.s^{-1}
$\dot{E}^o_{th}$	=	Rate of thermal energy outflow, J.s^{-1}
$\dot{E}^o_W$	=	Boundary isobaric pressure-work rate, J.s^{-1}
e	=	Mass-specific internal energy, J.kg^{-1}
h	=	Mass-specific static enthalpy, J.kg^{-1}
h_i	=	Mass-specific stagnation enthalpy, J.kg^{-1}
k	=	Thermal conductivity, W.m^{-1}.K^{-1}
$\mathbf{n}$	=	Unit normal vector
p	=	Static pressure, kg.m.s^{-2}
p_i	=	Stagnation pressure, kg.m.s^{-2}
$\mathbf{q}$	=	Heat flux by conduction, J.s^{-1}
r	=	Gas constant, J.kg^{-1}.K^{-1}
R	=	Inertial reference frame attached to the body
S_b	=	Body surface
S_o	=	Outer boundary of the control volume
S_w	=	Shockwave surface

*Ph.D. student, ONERA Department of Aerodynamics, Aeroelasticity, Acoustics, ilyes.berhouni@onera.fr.
†Research Scientist, Ph.D., ONERA Department of Aerodynamics, Aeroelasticity, Acoustics, didier.bailly@onera.fr.
‡Research Scientist, Ph.D., ONERA Department of Aerodynamics, Aeroelasticity, Acoustics, ilias.petropoulos@onera.fr.

s = Mass-specific entropy, J.K^{-1}.kg^{-1}

T = Static temperature, K

T_i = Stagnation temperature, K

$\mathcal{V}$ = Control volume

$\mathbf{V}$ = $(V_\infty + u)\mathbf{x}$, $v\mathbf{y}$, $w\mathbf{z}$, Fluid velocity vector, m.s^{-1}

$\dot{\mathcal{X}}_c^o$ = Compressible exergy outflow through S_o, J.s^{-1}

$\dot{\mathcal{X}}_{cR}^o$ = Compressible exergy outflow through S_o computed for a reference state at rest in R, J.s^{-1}

$\dot{\mathcal{X}}_k^o$ = Rate of kinetic exergy outflow through S_o

$\dot{\mathcal{X}}_m^o$ = Rate of mechanical exergy outflow, J.s^{-1}

$\dot{\mathcal{X}}_{mr}^o$ = Rate of mechanically-recoverable exergy outflow through S_o, J.s^{-1}

$\dot{\mathcal{X}}_q^b$ = Rate of thermal exergy supplied by conduction through S_b, J.s^{-1}

$\dot{\mathcal{X}}_q^o$ = Rate of thermal exergy supplied by conduction through S_o, J.s^{-1}

$\dot{\mathcal{X}}_{tf}^b$ = Rate of exergy inflow to the control volume, J.s^{-1}

$\dot{\mathcal{X}}_{tfmr}^b$ = Mechanically-recoverable component of $\dot{\mathcal{X}}_{tf}^b$, J.s^{-1}

$\dot{\mathcal{X}}_{tf\delta s}^b$ = Thermally-recoverable component of $\dot{\mathcal{X}}_{tf}^b$, J.s^{-1}

$\dot{\mathcal{X}}_{th}^o$ = Rate of thermocompressible exergy outflow, J.s^{-1}

$\dot{\mathcal{X}}_{thse}^o$ = Mechanically-recoverable component of the thermocompressible exergy outflow, J.s^{-1}

$\dot{\mathcal{X}}_{\delta s}^o$ = Thermally-recoverable component of the thermocompressible exergy outflow, J.s^{-1}

$\dot{\mathcal{X}}_{tr}^b$ = Exergy difference due to the analysis being performed in a reference frame in translation, J.s^{-1}

$\dot{\mathcal{X}}_{tr,p}^o$ = Pressure component of $\dot{\mathcal{X}}_{tr}^b$, J.s^{-1}

χ_f = Mass-specific flow exergy, J.kg^{-1}

χ_s = Static component of specific exergy, J.kg^{-1}

γ = Gas specific heat ratio

$\delta(\ )$ = Perturbation of a quantity relative to the freestream, $= (\ ) - (\ )_\infty$

ρ = Density, kg.m^{-3}

$\overline{\overline{\tau}}$ = Viscous stress tensor, N

ϕ = Dissipation rate per unit volume, J.s^{-1}.m^{-3}

$(\ )_\infty$ = Quantity $(\ )$ at freestream conditions

$(\ )_{se}$ = Quantity $(\ )$ obtained after an isentropic expansion to the reference state pressure

∇ = Nabla operator

$[\![\ ]\!]$ = Discontinuous jump of a quantity

I. Introduction

The interest in the concept of exergy [1, 2] for the performance investigation of various systems in the field of aerodynamics has significantly grown over the last decades. Arntz et al. [3, 4] developed a method based on an exergy balance adapted to steady external aerodynamic analyses, which allows to perform a phenomenological decomposition of exergy fluxes in the system studied and provides a clear association between physical phenomena and reversible/irreversible exergy loss. This method was then used to investigate the performance of conventional and non-conventional configurations [4–9], as well as investigated from a numerical point of view numerically [10, 11]. Further work was performed in recent years to adapt the exergy balance method to experimental studies [12–14], flows resolved in rotating reference frames [15–17] and unsteady flow analyses [18–20]. Other works focused on the use of the exergy balance or metrics related to it alongside the power balance method developed by Drela [21] in order to define performance metrics adapted to the evaluation of possible boundary-layer ingestion benefits with different fuselage geometries, with or without heating [22, 23].

Still, the fine interpretation of complex effects requires a clearer physical decomposition of the exergy balance. A first step in this direction was recently performed concerning the influence of reference frame transformation (between a geocentric and a translating reference frame) on the analysis [20]. Others require further work, in particular concerning the decomposition of thermal and compressible effects contained in the thermocompressible (or static) exergy outflow [4, 20]. The latter is required for the quantification of the pure potential for mechanical work recovery (e.g. by a turbine) and the one that can only be recovered by means of thermal transfers associated to a Carnot machine (in the optimal case). Indeed, the commonly-used decomposition between mechanical and thermocompressible exergy outflows may lead to unintuitive results for specific cases for which thermal effects are expected to be negligible, yet thermocompressible exergy outflow is significant. Such a case was encountered by Aguirre [14], who used an alternative decomposition of the thermocompressible exergy outflow (also suggested by Arntz [4]) between a thermal and a pressure component. This decomposition was achieved by separating the density and temperature contributions in the entropy flux. It however raises concerns since having no entropy difference between the system and its dead state does not guarantee that the resulting thermal component is null. In other words, part of the exergy outflow could be considered to be convertible into mechanical work through thermal transfers, even without entropy generation. This inconsistency implies that this definition of the thermal exergy outflow is not guaranteed to exclude compressible effects that hold a potential for mechanical work extraction.

This paper aims at presenting a new method for the decomposition of the thermocompressible exergy outflow between a compressible and a purely thermal component, based on the work of Miller [24]. Sec. II details the exergy balance derived by Arntz et al. [3, 4] and the decompositions of thermocompressible exergy outflow suggested by Arntz et al. and used by Aguirre et al., alongside the concerns associated with these decompositions. In Sec. III, the method used by Miller to define the mechanical work potential of a system is presented, and its application to the

decomposition of the thermocompressible exergy outflow is detailed. New definitions for the purely mechanical (with a kinetic and a compressible contribution) and purely thermal exergy outflow are then proposed, alongside an analysis of the properties of the newly-defined thermal exergy outflow. The exergy balance decomposition is then reexpressed, and the decoupling between the impact of the reference state pressure and temperature on the balance is highlighted. The additional information provided by the new exergy balance decomposition is then detailed for the theoretical case of an isentropic flow in a converging nozzle. Conclusive remarks and perspectives regarding this new decomposition are finally detailed in Sec. IV.

II. Exergy balance for a reference frame in translation

A. System definition

The analysis is performed in a continuous control volume $\mathcal{V}$ limited by three surfaces noted S_o, S_b and S_w, as shown in Fig. 1. The surfaces S_o and S_b respectively correspond to an outer boundary and the aircraft surface, while S_w corresponds to a shockwave discontinuity. This volume is closed and its limits can be permeable, with a vector **n** normal to the surface and pointing outwards of the volume (i.e. towards the interior of the shockwave volume for S_w).

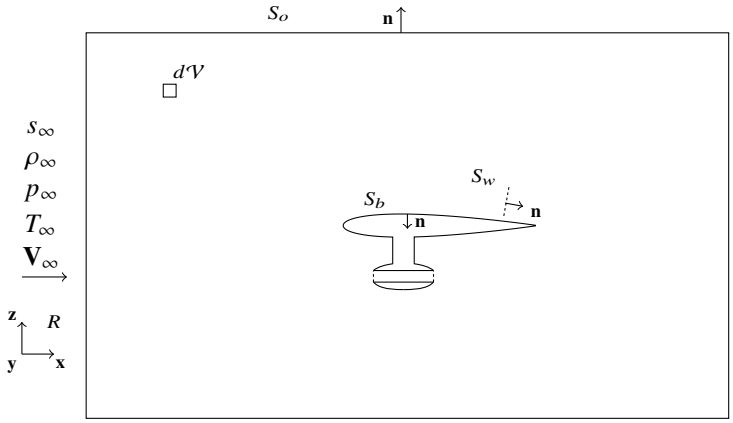

Fig. 1 2D cross section of a 3D control volume surrounding the aircraft as seen in R.

The system is thermodynamically open as it exchanges mass, work and heat with the surrounding fluid across its boundaries. The atmosphere is considered as a thermal and mechanical reservoir which also corresponds to the dead state in the exergy definition. The analysis is carried out in a reference frame R, assumed inertial, and the control volume is fixed in R with the fluid flowing in and out of it. R translates at the same velocity as the aircraft with respect to a geocentric reference frame, so the aircraft velocity is null whereas the atmosphere is considered to have a velocity $\mathbf{V}_\infty$. In this paper, a steady-state flow assumption is considered in the calculations.

B. Exergy balance

Exergy [2] quantifies the maximum mechanical work that can be extracted from a system while it evolves towards its dead state. For the investigation of a steady-state flow, it is relevant to work with the flow exergy defined for a reference state in motion as [20]:

$$\chi_f = \underbrace{\delta e + p_\infty \delta\left(\frac{1}{\rho}\right) - T_\infty \delta s}_{\chi_s} + \underbrace{\frac{1}{2}(\mathbf{V}-\mathbf{V}_\infty)\cdot(\mathbf{V}-\mathbf{V}_\infty)}_{KE} \underbrace{+\frac{\delta p}{\rho}}_{\text{Transfer power}} \tag{1}$$

where χ_s is the static exergy (which corresponds to static thermodynamic effects such as the system compression or expansion), KE is the perturbation kinetic energy (i.e. the kinetic energy in a reference frame for which the atmosphere is at rest) and the transfer power is the power setting the flow in motion (associated to a pressure difference). The last two terms are thus different from zero due to the flow being in motion. A balance of this quantity can be derived for the control volume in Fig. 1 by making use of the conservation equations and the entropy equation, performing a phenomenological decomposition (between static and dynamic effects) and finally a surface separation (in terms of near-field and far-field contributions). The fully-decomposed exergy balance obtained with this methodology is then [20]:

$$\dot{\mathcal{X}}^b_{tf} + \dot{\mathcal{X}}^b_q = \dot{\mathcal{X}}^b_{tr} + \dot{\mathcal{X}}^o_m + \dot{\mathcal{X}}^o_{th} + \dot{\mathcal{X}}^o_q + \dot{\mathcal{A}}_\phi + \dot{\mathcal{A}}_{\nabla T} + \dot{\mathcal{A}}_w \tag{2}$$

where:

- $\dot{\mathcal{X}}^b_{tf} = -\int_{S_b} \rho\left(\delta e + p_\infty \delta\left(\frac{1}{\rho}\right) - T_\infty \delta s\right)\mathbf{V}\cdot\mathbf{n}\,\mathrm{d}S - \int_{S_b}\left(\rho\frac{1}{2}V^2\mathbf{V} + ((p-p_\infty)\overline{\overline{I}} - \overline{\overline{\tau}})\cdot\mathbf{V}\right)\cdot\mathbf{n}\,\mathrm{d}S$ is referred to as the throughflow exergy, and represents the flux of exergy through permeable surfaces of S_b perceived in R, and the associated rate of work of surface forces.
- $\dot{\mathcal{X}}^b_q = -\int_{S_b}\left(1-\frac{T_\infty}{T}\right)\mathbf{q}\cdot\mathbf{n}\,\mathrm{d}S$ is the exergy transferred by thermal conduction through non-adiabatic parts of S_b.
- $\dot{\mathcal{X}}^b_{tr} = -\mathbf{V}_\infty\cdot\int_{S_b}(\rho\mathbf{V}\otimes\mathbf{V} + (p-p_\infty)\overline{\overline{I}} - \overline{\overline{\tau}})\cdot\mathbf{n}\,\mathrm{d}S + \int_{S_b}\frac{1}{2}V_\infty^2\rho\mathbf{V}\cdot\mathbf{n}\,\mathrm{d}S$ is an exergy difference appearing due to the frame of reference being in translation with respect to the geocentric reference frame in which exergy is defined [20]. It is composed of the variation of the work rate of surface forces and the kinetic energy difference associated to the translation of the reference frame.
- $\dot{\mathcal{X}}^o_m = \int_{S_o}\rho\frac{1}{2}(u^2+v^2+w^2)\mathbf{V}\cdot\mathbf{n}\,\mathrm{d}S + \int_{S_o}((p-p_\infty)\overline{\overline{I}} - \overline{\overline{\tau}})\cdot(\mathbf{V}-\mathbf{V}_\infty)\cdot\mathbf{n}\,\mathrm{d}S$ is the mechanical exergy flux, composed of the flux of kinetic perturbation exergy and the surface force rate of work linked to these velocity perturbations. Note that the above definition includes the viscous force rate of work [20], which was neglected and not included in the expression of the $\dot{\mathcal{X}}^o_m$ term in previous works [4, 21].
- $\dot{\mathcal{X}}^o_{th} = \int_{S_o}\rho\left(\delta e + p_\infty\delta\left(\frac{1}{\rho}\right) - T_\infty\delta s\right)\mathbf{V}\cdot\mathbf{n}\,\mathrm{d}S$ is the static exergy flux (also referred to as thermocompressible exergy flux). Note that this definition differs from [4], where mass flow variation on S_o was neglected.

- $\dot{\mathcal{X}}_q^o = \int_{S_o} \left(1 - \frac{T_\infty}{T}\right) \mathbf{q} \cdot \mathbf{n} \, \mathrm{d}S$ is the exergy transferred by thermal conduction through S_o.
- $\dot{\mathcal{A}}_\phi = \int_{\mathcal{V}} \frac{T_\infty}{T} \phi \, \mathrm{d}\mathcal{V}$ is the viscous anergy generation by viscous effects.
- $\dot{\mathcal{A}}_{\nabla T} = \int_{\mathcal{V}} \frac{T_\infty}{T^2} k (\nabla T)^2 \, \mathrm{d}\mathcal{V}$ is the thermal anergy generation by thermal mixing.
- $\dot{\mathcal{A}}_w = T_\infty \int_{S_w} [\![\frac{1}{T} \mathbf{q} + \rho \delta s \mathbf{V}]\!] \cdot \mathbf{n} \, \mathrm{d}S$ is the wave anergy generation due to the presence of shockwave(s).

Note that in Eq. (2), the exergy outflow is rather decomposed between static (as the expression for χ_s is conserved in $\dot{\mathcal{X}}_{th}^o$) and dynamic contributions (as the transfer power and perturbation kinetic energy are included in $\dot{\mathcal{X}}_m^o$). Nevertheless, the nomenclature proposed by Arntz et al. [3, 4] (i.e. thermocompressible and mechanical components) is conserved for a clearer link to previous works. In the following, the viscous contribution to the mechanical exergy outflow will be neglected for simplicity. If it were to be considered as non-negligible, the only difference in the following developments would be the inclusion of the viscous-force integral as is in the final expressions. The mechanical exergy outflow can be decomposed as [4, 21]:

$$\dot{\mathcal{X}}_m^o = \underbrace{\int_{S_o} \rho \frac{1}{2} u^2 \mathbf{V} \cdot \mathbf{n} \, \mathrm{d}S}_{\dot{E}_u^o} + \underbrace{\int_{S_o} \rho \frac{1}{2} (v^2 + w^2) \mathbf{V} \cdot \mathbf{n} \, \mathrm{d}S}_{\dot{E}_{vw}^o} + \underbrace{\int_{S_o} (p - p_\infty)(\mathbf{V} - \mathbf{V}_\infty) \cdot \mathbf{n} \, \mathrm{d}S}_{\dot{E}_p^o} \tag{3}$$

where $\dot{E}_u^o$ and $\dot{E}_{vw}^o$ represent respectively the flux of longitudinal and transversal kinetic perturbation energy, while $\dot{E}_p^o$ corresponds to the associated boundary-pressure rate of work. A decomposition was also suggested for the thermocompressible exergy outflow as [4]:

$$\dot{\mathcal{X}}_{th}^o = \underbrace{\int_{S_o} \rho \delta e \mathbf{V} \cdot \mathbf{n} \, \mathrm{d}S}_{\dot{E}_{th}^o} + \underbrace{\int_{S_o} \rho p_\infty \delta \left(\frac{1}{\rho}\right) \mathbf{V} \cdot \mathbf{n} \, \mathrm{d}S}_{\dot{E}_W^o} - \underbrace{\int_{S_o} T_\infty \rho \delta s \mathbf{V} \cdot \mathbf{n} \, \mathrm{d}S}_{\dot{A}^o} \tag{4}$$

where $\dot{E}_{th}^o$ is the thermal energy outflow, $\dot{E}_W^o$ is the rate of isobaric surroundings work and $\dot{A}^o$ is the outflow rate of anergy.

Decomposing the overall exergy outflow into $\dot{\mathcal{X}}_m^o$ and $\dot{\mathcal{X}}_{th}^o$ does have a physical sense, as the mechanical exergy outflow can be linked to the induced drag for an inviscid low-speed flow around a three-dimensional body [4, 21]. However, from a thermodynamic point of view, it does not correspond to a separation between mechanical and thermal effects but rather to a separation between dynamic and static thermodynamic effects (cf. above discussion). Compressible contributions which hold a potential for direct mechanical work extraction are present in both the mechanical ($\dot{E}_p^o$) and thermocompressible (part of $\dot{E}_{th}^o$ and $\dot{E}_W^o$) exergy outflows. Thus, part of $\dot{\mathcal{X}}_{th}^o$ can be directly converted to mechanical work by means of a mechanical device (e.g. a turbine) using the fluid pressure variations with respect to its dead state. Another part of $\dot{\mathcal{X}}_{th}^o$ can only be recovered by means of thermal processes with thermal machines (Carnot machines in the optimal case) using the system either as a hot or cold thermal source. Note that even in the optimal case of

a Carnot machine, the mechanical work extraction from thermal transfers can be done reversibly but not at constant entropy, making heat an energy source of lower quality with respect to mechanical energy. To tackle the concerns associated with the separation between dynamic and static effects, Arntz [4] proposed an alternative decomposition of the thermocompressible exergy outflow as:

$$\dot{\mathcal{X}}^o_{th} = \underbrace{\int_{S_o} \rho c_v T \left(1 - \frac{T_\infty}{T} ln\left(\frac{T}{T_\infty}\right)\right) \mathbf{V}\cdot\mathbf{n}\,\mathrm{d}S - \int_{S_o} \rho c_v T_\infty \mathbf{V}\cdot\mathbf{n}\,\mathrm{d}S}_{\dot{\mathcal{X}}^o_{th_T}} + \underbrace{\int_{S_o} p_\infty \left(1 - \frac{\rho}{\rho_\infty} ln\left(\frac{\rho_\infty}{\rho}\right)\right) \mathbf{V}\cdot\mathbf{n}\,\mathrm{d}S - \int_{S_o} \rho r T_\infty \mathbf{V}\cdot\mathbf{n}\,\mathrm{d}S}_{\dot{\mathcal{X}}^o_{th_P}} \tag{5}$$

where $\dot{\mathcal{X}}^o_{th_T}$ and $\dot{\mathcal{X}}^o_{th_P}$ are referred to as pure temperature and pressure components. This decomposition was then selected by Aguirre [14] to tackle inconsistencies in the applications investigated. It is achieved by expressing entropy as a function of static temperature and density and separating these components between $\dot{\mathcal{X}}^o_{th_T}$ and $\dot{\mathcal{X}}^o_{th_P}$. The pressure term was then considered a pure mechanical contribution by Aguirre [14] and added to the mechanical exergy outflow. A consequence of this decomposition is that the entropy flux no longer appears clearly. Additionally, if $s = s_\infty$, there is no guarantee that the thermal component equals zero, which should be the case as the absence of entropy change in a system compared to its dead state should correspond to the absence of a mechanical work potential from thermal exchanges.

The next section proposes a new approach for the decomposition of the thermocompressible and mechanical exergy outflow based on the approach of Miller [24], used for the definition of the mechanical work potential (also referred to as euergy [25, 26]).

III. Derivation of a new exergy balance decomposition based on an optimal path for mechanical work recovery

A. Mechanical work potential

Miller [24] suggested a new approach to quantify the potential of mechanical work that can be extracted from a system using a turbine. It consists in fixing an optimal path for mechanical work extraction through the processes under which the system goes back to its dead state. This path is composed of an isentropic expansion bringing the fluid to the dead state stagnation pressure $p_{i\infty}$ (with an associated temperature $T_{i,se}$) followed by reversible heat exchanges which bring the fluid back to the dead state temperature. This optimal path applied to a system at (p_{i1},T_{i1}) is illustrated with a Mollier diagram in Fig. 2.

The mechanical work that can be extracted from the isentropic process corresponds to the path $1 \rightarrow 2, se$ and is referred to as flow mechanical work potential by Miller [24]. It corresponds to the work that could be extracted from the system by an isentropic turbine exhausting to the dead state stagnation pressure. The expressions for the stagnation and

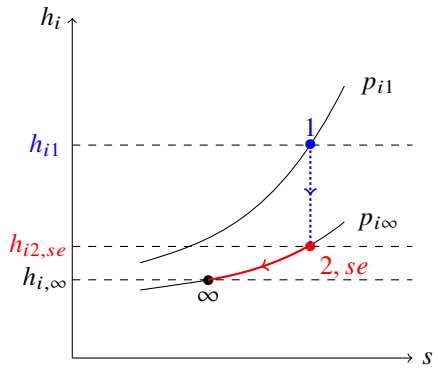

Fig. 2 Mollier diagram corresponding to an isentropic expansion followed by reversible heat exchanges.

static temperature associated to the state 2, se in Fig. 2 are obtained with the isentropic relations:

$$\frac{T_{i,se}}{T_i} = \left(\frac{p_{i\infty}}{p_i}\right)^{\frac{\gamma-1}{\gamma}} \qquad \frac{T_{se}}{T} = \left(\frac{p_\infty}{p}\right)^{\frac{\gamma-1}{\gamma}} \tag{6}$$

The work associated to the path 2, $se \rightarrow \infty$ is then referred to as the flow thermal work potential, which corresponds to the work that can be extracted from the system by using a Carnot machine coupled to the system and to a reservoir with a stagnation temperature $T_{i\infty}$.

A mechanical work potential balance was derived by Miller with this approach, and was used to analyse the additional potential for mechanical work recovery linked to thermal effects in the control volume studied (referred to as thermal creation in Miller's work). The flow thermal work potential on the other hand is not quantified by Miller's method, as is was argued that this component is of little interest to turbine designers. More recently, Jardine and Miller [25, 26] argued that the mechanical work potential should be considered as more relevant than exergy for turbine designers, as the inclusion of purely thermal exergy in the definition leads to discrepancies in the prediction of cooled turbine efficiency.

B. Application to the derivation of a new decomposition of the exergy balance

1. Decomposition of the thermocompressible exergy outflow

The exergy balance allows to quantify the maximum mechanical work that can be extracted from a system by means of reversible heat exchanges and isentropic mechanical processes. The order of the processes involved is not however fixed. There exists therefore an infinity of theoretical paths which can lead to the conversion of exergy outflow into mechanical work. This led to the decomposition of Arntz et al. [3, 4] between dynamic and static effects, discussed in Sec. II. The aim of this section is to set an optimal path for mechanical work recovery, as done by Miller [24] for the definition of mechanical work potential. This approach does not allow a further decomposition of mechanical exergy outflow $\dot{\mathcal{X}}_m^o$ (cf. Eq. (2)), as this component is already fully recoverable by a turbine. However, setting an optimal path for mechanical work recovery allows to perform a new decomposition of the thermocompressible exergy

outflow $\dot{\mathcal{X}}^o_{th}$ into a compressible (recoverable by a turbine, part of the $1 \rightarrow 2, se$ path) and a purely thermal contribution (i.e. thermally-recoverable, $2, se \rightarrow \infty$ path), as:

$$\dot{\mathcal{X}}^o_{th} = \dot{\mathcal{X}}^o_{thse} + \dot{\mathcal{X}}^o_{\delta s} \tag{7}$$

where:

$$\dot{\mathcal{X}}^o_{thse} = \int_{S_o} \rho c_v (T - T_{se}) \mathbf{V} \cdot \mathbf{n} \, \mathrm{d}S + \int_{S_o} \rho p_\infty \left(\frac{1}{\rho} - \frac{1}{\rho_{se}} \right) \mathbf{V} \cdot \mathbf{n} \, \mathrm{d}S \tag{8}$$

$$\dot{\mathcal{X}}^o_{\delta s} = \int_{S_o} \rho c_v (T_{se} - T_\infty) \mathbf{V} \cdot \mathbf{n} \, \mathrm{d}S + \int_{S_o} \rho p_\infty \left(\frac{1}{\rho_{se}} - \frac{1}{\rho_\infty} \right) \mathbf{V} \cdot \mathbf{n} \, \mathrm{d}S - \int_{S_o} \rho T_\infty (s - s_\infty) \mathbf{V} \cdot \mathbf{n} \, \mathrm{d}S \tag{9}$$

This is equivalent to setting an optimal path for the conversion of exergy outflow into mechanical work (optimal in the sense that the potential of conversion by surface forces and kinetic energy is considered more relevant than thermal transfers). The contributions of the different exergy balance components in this path are illustrated using a Mollier diagram in Fig. 3.

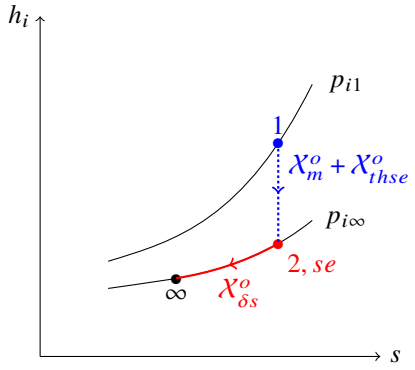

Fig. 3 Representation of the new thermocompressible exergy outflow decomposition on a Mollier diagram.

The term $\dot{\mathcal{X}}^o_{thse}$ represents the mechanically-recoverable part of the overall thermocompressible exergy outflow. It is referred to as a mechanical contribution in the sense that it creates a potential for mechanical work linked to a higher stagnation pressure, which can be directly recovered by a mechanical device (e.g. a turbine). $\dot{\mathcal{X}}^o_{\delta s}$ on the other hand is the thermally-recoverable portion of $\dot{\mathcal{X}}^o_{th}$ that is only recoverable by means of thermal transfers (ideally by a Carnot machine).

2. Derivation of a new expression for the mechanical exergy outflow

The mechanical component of the thermocompressible exergy outflow $\dot{\mathcal{X}}^o_{thse}$ can be included into the mechanical exergy outflow alongside $\dot{E}^o_p$ as:

$$\dot{\mathcal{X}}^o_c = \dot{E}^o_p + \dot{\mathcal{X}}^o_{thse} = \int_{S_o} (p - p_\infty)(\mathbf{V} - \mathbf{V}_\infty) \cdot \mathbf{n} \, \mathrm{d}S + \int_{S_o} \rho c_v (T - T_{se}) \mathbf{V} \cdot \mathbf{n} \, \mathrm{d}S + \int_{S_o} \rho p_\infty \left(\frac{1}{\rho} - \frac{1}{\rho_{se}} \right) \mathbf{V} \cdot \mathbf{n} \, \mathrm{d}S \tag{10}$$

$\dot{\mathcal{X}}_c^o$ represents the exergy outflow linked to the compressibility of the fluid that can be directly converted into mechanical work. Note that $\dot{\mathcal{X}}_c^o = \dot{E}_c^o$, as this term is mechanical and thus theoretically completely convertible into mechanical work. As p_∞ is constant and the perfect gas law gives $\frac{p_\infty}{\rho_{se}} = rT_{se}$, it is further transformed into:

$$\dot{\mathcal{X}}_c^o = \underbrace{-\int_{S_o}(p-p_\infty)\mathbf{V}_\infty\cdot\mathbf{n}\,\mathrm{d}S}_{\dot{\mathcal{X}}_{tr,p}^o} + \underbrace{\int_{S_o}\rho(h-h_{se})\mathbf{V}\cdot\mathbf{n}\,\mathrm{d}S}_{\dot{\mathcal{X}}_{cR}^o} \tag{11}$$

where $\dot{\mathcal{X}}_{tr,p}^o$ is the rate of work done by pressure forces on S_o associated to the reference frame translation [20] and $\dot{\mathcal{X}}_{cR}^o$ is the compressible exergy outflow perceived in R. Note that $\dot{\mathcal{X}}_{cR}^o$ can be rewritten using Eq. (6) as $\dot{\mathcal{X}}_{cR}^o = \int_{S_o}\rho c_p T(1-(p_\infty/p)^{(\gamma-1)/\gamma})\mathbf{V}\cdot\mathbf{n}\,\mathrm{d}S$.

Considering the above relations, the mechanical exergy outflow can finally be redefined as:

$$\dot{\mathcal{X}}_{mr}^o = \dot{E}_u^o + \dot{E}_{vw}^o + \dot{E}_p^o + \dot{\mathcal{X}}_{thse}^o \tag{12}$$

$$= \underbrace{\int_{S_o}\rho\frac{1}{2}(u^2+v^2+w^2)\mathbf{V}\cdot\mathbf{n}\,\mathrm{d}S}_{\dot{\mathcal{X}}_k^o} + \dot{\mathcal{X}}_c^o \tag{13}$$

where $\dot{\mathcal{X}}_k^o$ is the kinetic perturbation exergy outflow. The above term will be referred to as mechanically-recoverable exergy outflow in the following, as it contains all kinetic and compressible effects that hold potential for direct mechanical work recovery, with reversible transfers occurring between $\dot{\mathcal{X}}_k^o$ and $\dot{\mathcal{X}}_c^o$. The different levels of decomposition of the newly defined mechanically-recoverable exergy outflow are then:

$$\dot{\mathcal{X}}_{mr}^o = \dot{\mathcal{X}}_k^o + \underbrace{\dot{E}_p^o + \dot{\mathcal{X}}_{thse}^o}_{} \tag{14}$$

$$= \dot{\mathcal{X}}_k^o + \underbrace{\dot{\mathcal{X}}_{tr,p}^o + \dot{\mathcal{X}}_{cR}^o}_{} \tag{15}$$

$$= \dot{\mathcal{X}}_k^o + \dot{\mathcal{X}}_c^o \tag{16}$$

3. Properties of the newly defined thermal exergy outflow

The thermally-recoverable component of $\dot{\mathcal{X}}_{th}^o$ (cf. Eq. (9)) can also be rewritten as:

$$\dot{\mathcal{X}}_{\delta s}^o = \int_{S_o}\rho c_p(T_{se}-T_\infty)\mathbf{V}\cdot\mathbf{n}\,\mathrm{d}S - \int_{S_o}T_\infty\rho(s-s_\infty)\mathbf{V}\cdot\mathbf{n}\,\mathrm{d}S \tag{17}$$

Since $\dot{\mathcal{X}}_{\delta s}^o$ corresponds to the path 2, $se\to\infty$ (cf. Fig. 3), the entropy difference of the second integrand can be

expressed as:

$$s - s_\infty = s_{se} - s_\infty = c_p \left(ln\left(\frac{T_{se}}{T_\infty}\right) - \frac{\gamma - 1}{\gamma} \cancel{ln\left(\frac{p_{se}}{p_\infty}\right)} \right) \tag{18}$$

where $s_{se} = s_1$ and $p_{se} = p_\infty$.

Using Eq. (18), the ratio between T_{se} and T_∞ is expressed as:

$$\frac{T_{se}}{T_\infty} = e^{\frac{s - s_\infty}{c_p}} \tag{19}$$

which is injected into Eq. (17):

$$\dot{\mathcal{X}}^o_{\delta s} = \int_{S_o} \rho c_p T_\infty \left(e^{\frac{s - s_\infty}{c_p}} - 1 \right) \mathbf{V} \cdot \mathbf{n} \, \mathrm{d}S - \int_{S_o} T_\infty \rho (s - s_\infty) \mathbf{V} \cdot \mathbf{n} \, \mathrm{d}S \tag{20}$$

The above equation defines the purely thermal exergy outflow linked to an entropy variation of the system with respect to its reference state. Its two components can then be grouped as:

$$\dot{\mathcal{X}}^o_{\delta s} = \int_{S_o} \rho c_p T_\infty \left(e^{\frac{s - s_\infty}{c_p}} - \left(1 + \frac{s - s_\infty}{c_p} \right) \right) \mathbf{V} \cdot \mathbf{n} \, \mathrm{d}S \tag{21}$$

As $e^x \geq 1 + x \ \ \forall x \in \mathbb{R}$, the integrand of the newly defined thermal exergy is always positive and $\dot{\mathcal{X}}^o_{\delta s} = 0$ for $s = s_\infty$. This highlights that any entropy difference holds a potential for mechanical work recovery by using a Carnot machine (the system being either the hot or cold source depending on its temperature being higher or lower than T_∞). Additionally, the higher the temperature difference between the current and dead state (i.e. the higher the entropy difference), the higher the mechanical work recovery potential (although the integrand value is of second order with respect to the anergy generation). Note that such an expression was also obtained in a scalar approach by Ruiz for the thermal component of the flow exergy [27].

4. Exergy balance corresponding to the new decomposition

In addition, $\dot{\mathcal{X}}^b_{tf}$ can be decomposed between its thermal and mechanical (kinetic and compressible) components as:

$$\dot{\mathcal{X}}^b_{tf} = \underbrace{- \int_{S_b} \rho c_p (T - T_{se}) \mathbf{V} \cdot \mathbf{n} \, \mathrm{d}S - \int_{S_b} \rho \frac{1}{2} V^2 \mathbf{V} \cdot \mathbf{n} \, \mathrm{d}S}_{\dot{\mathcal{X}}^b_{tfmr}} \underbrace{- \int_{S_b} \rho c_p T_\infty \left(e^{\frac{s - s_\infty}{c_p}} - \left(1 + \frac{s - s_\infty}{c_p} \right) \right) \mathbf{V} \cdot \mathbf{n} \, \mathrm{d}S}_{\dot{\mathcal{X}}^b_{tf\delta s}} \tag{22}$$

The newly-decomposed exergy balance (to be compared with Eq. (2)) is then expressed as:

$$\dot{\mathcal{X}}^b_{tfmr} + \dot{\mathcal{X}}^b_{tf\delta s} + \dot{\mathcal{X}}^b_q = \dot{\mathcal{X}}^b_{tr} + \dot{\mathcal{X}}^o_{mr} + \dot{\mathcal{X}}^o_{\delta s} + \dot{\mathcal{X}}^o_q + \dot{\mathcal{A}}_\phi + \dot{\mathcal{A}}_{\nabla T} + \dot{\mathcal{A}}_w \tag{23}$$

Note that this new form of the exergy balance actually corresponds to a decomposition relative to the reference state variables. Indeed, as $T_{se} = f(p_\infty)$, two groups of terms can be identified with respect to their dependence on the reference state variables:

$$\begin{cases} \dot{\mathcal{X}}^b_{tfmr}, \dot{\mathcal{X}}^b_{tr}, \dot{\mathcal{X}}^o_{mr} = f(p_\infty, V_\infty) & (24) \\ \dot{\mathcal{X}}^b_{tf\delta s}, \dot{\mathcal{X}}^b_{q}, \dot{\mathcal{X}}^o_{\delta s}, \dot{\mathcal{X}}^o_{q}, \dot{\mathcal{A}}_\phi, \dot{\mathcal{A}}_{\nabla T}, \dot{\mathcal{A}}_w = f(T_\infty, s_\infty) & (25) \end{cases}$$

The dependency of the various terms is actually an indicator as to how the components are generated (in the case of anergy) or are/can be recovered (in the case of exergy outflow components). The components corresponding to Eq. (24) hold a potential for mechanical work recovery in terms of pressure and kinetic energy variations by means of a mechanical device (ideally by an adiabatic turbine exhausting at p_∞). The ones appearing in Eq. (25) rather correspond to the potential for mechanical work extraction in terms of temperature (and thus entropy) variations by means of a thermal machine connected to a cold/hot source (ideally a Carnot machine).

The efficiency improvement of mechanical devices could focus on components which depend on p_∞ and V_∞, as these are representative of the maximum mechanical work that can be extracted without a thermal machine. From this perspective, while anergy components are already traditionally viewed as an irreversible loss, $\dot{\mathcal{X}}^o_{\delta s}$ should be considered as a non-recoverable exergy outflow. This reasoning might also provide an answer to concerns expressed by Miller and Jardine [24–26] in the field of turbine performance evaluation, which led to the development of the mechanical work potential. Indeed, these authors argue that exergy is not specific enough as it always measures the work that can be extracted by a combination of an adiabatic turbine and a thermal machine which overall brings the fluid at (p_∞, T_∞). The decomposition of Eq. (23) however gives a clear means of dissociating these processes with an increased flexibility for the designer as to what should be considered as loss (theoretically irreversible or not) and what should be considered as a possible improvement for the system. The interest of this decomposition is not however limited to internal configurations, as it might also address the difficulty of interpreting significant variations of $\dot{\mathcal{X}}^o_{th}$ in cases that do not involve thermal exchanges (e.g. such as those encountered in [14]). In such cases, the benefit of Eq. (23) is the guarantee that $\dot{\mathcal{X}}^o_{\delta s}$ is null when the entropy of the system is the same as the one in its dead state. Transfers between velocity and pressure are then all contained in $\dot{\mathcal{X}}^o_{mr}$ and $\dot{\mathcal{X}}^b_{tr}$, which represent the actual mechanical work that can be extracted by a classical turbine-type device. This advantage is further illustrated in Sec. III.C for the schematic case of an isentropic internal flow encountering a cross-section reduction (case of a converging nozzle), for which thermocompressible exergy is transformed into kinetic exergy. Note that Eq. (23) should also be more practical than Eq. (2) when evaluating the efficiency of boundary-layer ingestion systems, which may not possess any means of converting the $\dot{\mathcal{X}}^o_{\delta s}$ component into mechanical work. It is however expected to be of a similar practical use as the original decomposition of Eq. (2) in cases for which $\dot{\mathcal{X}}^o_{th}$ is negligible. It should finally be noted that since the new formulation presented in this paper only corresponds to a different decomposition of recoverable exergy outflows (i.e. $\dot{\mathcal{X}}^o_{m} + \dot{\mathcal{X}}^o_{th} = \dot{\mathcal{X}}^o_{mr} + \dot{\mathcal{X}}^o_{\delta s}$), the link

established by Drela between $\dot{\mathcal{X}}^o_m$ and induced drag remains valid under the same assumptions (integration on a Trefftz plane for low-speed incompressible flow outside of propulsion plumes and viscous wakes).

C. Theoretical case of an isentropic flow in a converging nozzle at rest

The case of an isentropic nozzle (illustrated in Fig. 4) is selected to highlight the differences between the exergy balance decompositions corresponding to Eqs. (2) and (23).

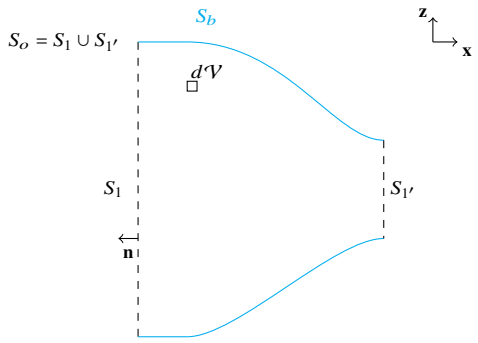

Fig. 4 2D cross section of a 3D control volume representative of a converging nozzle.

The same assumptions that were formulated in Sec. II are considered. In this case, the wall slip condition is expressed as $\mathbf{V} \cdot \mathbf{n} = 0$ (i.e. $\dot{\mathcal{X}}^b_{tf} = 0$) and, as the walls are adiabatic, $\dot{\mathcal{X}}^b_q = 0$. Additionally, the exergy flux by thermal conduction through S_o is assumed negligible, giving $\dot{\mathcal{X}}^o_q = 0$. The nozzle is assumed to be at rest for simplicity (i.e. $\mathbf{V}_\infty = \mathbf{0}$), thus $\dot{\mathcal{X}}^b_{tr} = 0$. As the flow is assumed to be isentropic, there is no anergy generated in the control volume. The dynamic/static and mechanical/thermal exergy balance decompositions from Eqs. (2) and (23) are then respectively reduced to:

$$0 = \dot{\mathcal{X}}^o_m + \dot{\mathcal{X}}^o_{th} \qquad 0 = \dot{\mathcal{X}}^o_{mr} + \dot{\mathcal{X}}^o_{\delta s} \tag{26}$$

The above equations are then rewritten to separate the fluxes through S_1 and $S_{1'}$ (e.g. $\dot{\mathcal{X}}^o_m = \dot{\mathcal{X}}^o_{m1} + \dot{\mathcal{X}}^o_{m1'}$):

$$-\dot{\mathcal{X}}^o_{m1} - \dot{\mathcal{X}}^o_{th1} = \dot{\mathcal{X}}^o_{m1'} + \dot{\mathcal{X}}^o_{th1'} \tag{27}$$

$$-\dot{\mathcal{X}}^o_{mr1} - \dot{\mathcal{X}}^o_{\delta s1} = \dot{\mathcal{X}}^o_{mr1'} + \dot{\mathcal{X}}^o_{\delta s1'} \tag{28}$$

The negative signs on fluxes through S_1 are due to the convention that the normal vector is oriented towards the exterior of the control volume. The decomposition by Arntz [4] might prove to be non-straightforward when trying to quantify the maximum mechanical work that could be directly extracted by an isentropic turbine for this system. To highlight this aspect, let us consider a system composed of an isentropic turbine exhausting at p_∞, associated to n reversible heat exchangers which are connected to Carnot machines (here using the atmosphere as a hot/cold source). This system is illustrated in Fig. 5 where $\dot{W}_{mt}$ represents the mechanical work extracted by the turbine and $\dot{W}_{mck}$

represents the work extracted by the k-th Carnot machine through the thermal transfers $\dot{Q}_{ck}$ and $\dot{Q}_{\infty k}$.

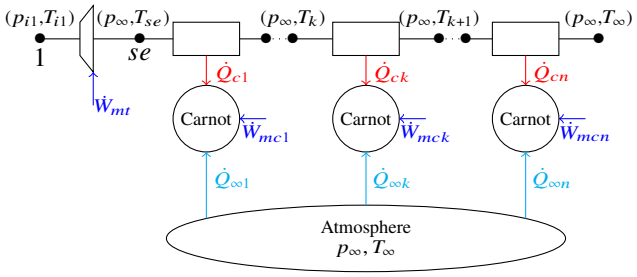

Fig. 5 Optimal system for mechanical work extraction.

By choosing this particular mechanical work extraction system, the processes involved are fixed and the resulting path corresponds to the one fixed by Miller [24] (cf. Fig. 2). Note that in this case the dead state is the atmosphere considered at rest, i.e. $p_{i\infty} = p_\infty$ and $T_{i\infty} = T_\infty$. Let us now assume that the above device is connected either to S_1 (with the flow in the corresponding state noted 1) or $S_{1'}$ (with the corresponding state $1'$). The Mollier diagrams that would be obtained by considering the decomposition of Eq. (27) are plotted in Fig. 6.

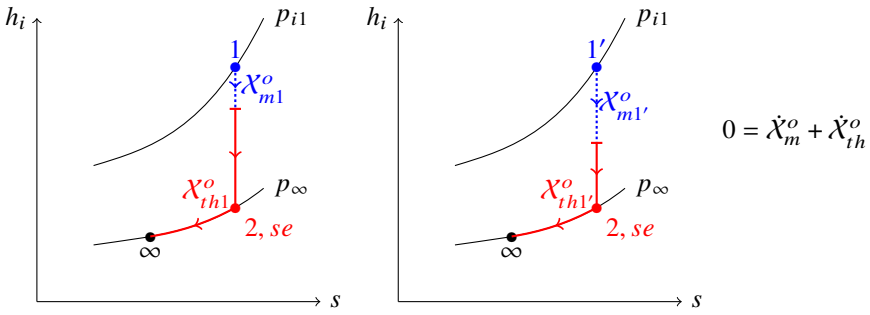

Fig. 6 Mollier diagram corresponding to the process described in Fig. 5 for the fluid state 1 (left) and $1'$ (right), considering the exergy balance decomposition of Arntz et al.

Considering that the state 1 or $1'$ of the system has no impact on the starting point in the Mollier diagrams, the only modification appears in the values of the phenomenological components of the exergy balance. Due to the cross-section reduction, part of the thermocompressible exergy is progressively converted into kinetic (and thus mechanical) exergy. The sum of the mechanical and thermocompressible exergy however remains constant between S_1 and $S_{1'}$ as no exergy is added or destroyed in the control volume considered. Fig. 6 highlights that the part of the thermocompressible exergy purely associated to heat transfers (and thus entropy) is not affected by the section reduction. The decomposition of the thermocompressible exergy of Eq. (4) is not however practical in terms of separating the mechanically- and thermally-recoverable contributions, leading to an uncertainty in the quantification of the exergy that can be extracted by a turbine device. The decomposition introduced by Arntz et al. and further used by Aguirre (cf. Eq. (5)) could be investigated, but the corresponding definition of thermal exergy $\dot{X}^o_{th_T}$ cannot adequately account for the thermal transfers involved. Indeed, if a system with no entropy difference with respect to its dead state was considered, there should be no

potential for mechanical work recovery due to thermal transfers, yet this is not guaranteed for the definition of Eq. (5).

The same Mollier diagrams are then plotted with a representation of the new exergy balance decomposition (cf. Eq. (28)). In this case, both $\mathcal{X}^o_{\delta s}$ and the sum $\mathcal{X}^o_{mr} = \mathcal{X}^o_k + \mathcal{X}^o_c$ are constant between S_1 and $S_{1'}$ due to the flow being isentropic and the reference state being at rest. No reversible transfers occur between the newly-defined thermal and mechanical exergy outflows due to the proposed decomposition. This is because $\mathcal{X}^o_{mr}$ only depends on the stagnation enthalpy (i.e. vertical position) of the flow state in Fig. 7, whereas the value of $\dot{\mathcal{X}}^o_{\delta s}$ only varies with its entropy (i.e. the horizontal position). It is therefore possible to distinguish between the mechanical work that can be extracted from the flow by a turbine-type device and the work that can be extracted by means of heat exchangers coupled to external thermal machines. In the case where the entropy of the system equals its dead state entropy, there is no potential for mechanical work recovery by the use of heat exchangers and $\mathcal{X}^o_{\delta s} = 0$, consistently with Eq. (21).

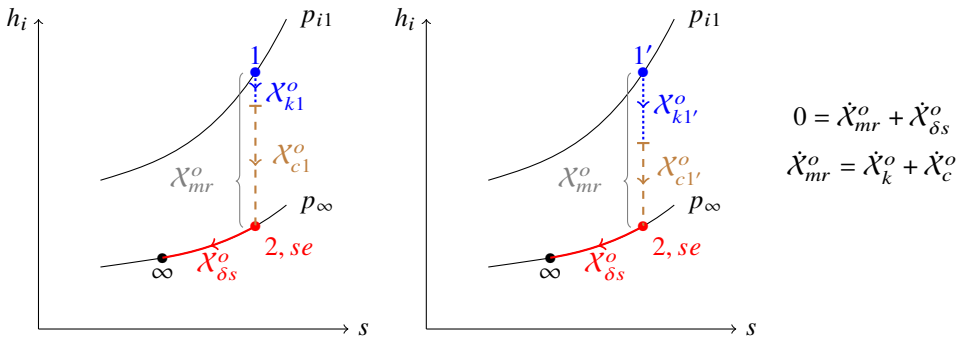

Fig. 7 Mollier diagram corresponding to the process described in Fig. 5 for the fluid state 1 (left) and 1′ (right).

IV. Conclusion and perspectives

This work proposes a new decomposition of the exergy balance currently in use for external aerodynamic applications [3, 4, 20], aiming at a clearer separation between mechanical and thermal contributions. This is done by adapting an approach suggested by Miller [24], which consists in fixing an optimal path for mechanical work extraction by a turbine. The method used to separate the thermocompressible exergy outflow into a compressible and a thermal part is first presented in detail. The compressible part is then added to the pressure-related component of the mechanical exergy outflow to obtain a compressible exergy outflow term, which in turn allows to define an overall mechanically-recoverable exergy outflow term. The properties of the new mechanical and thermal exergy outflows are then investigated theoretically, and arguments are presented for the relevance of this new decomposition. In particular, the present work highlights the guaranteed positivity and the null value of the new thermal exergy outflow integrand for $\delta s = 0$, as well as the decoupling of the reference state mechanical and thermal properties in the final exergy balance decompositions. This last step also provides a potential solution to concerns expressed previously on the use of exergy in turbine performance analysis [24, 25]. Finally, the advantages of the new decomposition compared to previous works is analysed on the

theoretical case of an isentropic flow in a converging nozzle. The new decomposition proposed is particularly (but not only) useful for internal flows with a non-negligible thermocompressible exergy outflow. Concerning external aerodynamics, future works could also explore a possible link between induced drag and mechanically-recoverable exergy outflow in a compressible regime. In general, power-balance methodologies perceive reversible transfers due to compressibility only as a variation of mechanical energy in the flow. In order to distinguish irreversible mechanical energy variations from reversible ones, such approaches may require integrations far from the body in order to limit reversible contributions, or resort to approximations under additional assumptions [23]. Exergy-balance methods on the other hand explicitly account for both mechanical and thermal effects. In particular, the formulation presented in this paper allows the complete inclusion of compressible reversible transfers within the mechanically-recoverable exergy outflow component, providing therefore a clearer separation of these with respect to transfers associated to irreversible effects. The proposed decomposition could thus also prove to be useful for cases that do not involve significant thermal exchanges, but require analyses in regions of significant reversible transfers between the balance components due to compressibility. Overall, it would be interesting to apply such a decomposition to the exergy balance adapted to rotating frames of reference [16] in order to investigate systems such as a compressor or a turbine rotor. The steps involved would be exactly the same as the ones presented in this paper, but with fluxes expressed in a rotating reference frame. The new decomposition is expected to provide additional elements of investigation for the performance analysis of a cooled turbine, since the thermal exergy (which cannot be directly recovered by this device) could be isolated and quantified as a loss.

Acknowledgments

The work presented in this paper was funded by the French Directorate General for Civil Aviation (DGAC) through the SUBLIME convention.

References

[1] Kotas, T. J., "Chapter 4 - Exergy analysis of simple processes," *The Exergy Method of Thermal Plant Analysis*, Elsevier, 1985, pp. 99–161. https://doi.org/10.1016/b978-0-408-01350-5.50011-8.

[2] Çengel, Y. A., and Boles, M. A., "Chapter 8 - Exergy," *Thermodynamics: An Engineering Approach.*, 2015. 8th edition, New York: McGraw-Hill.

[3] Arntz, A., Atinault, O., and Merlen, A., "Exergy-Based Formulation for Aircraft Aeropropulsive Performance Assessment: Theoretical Development," *AIAA Journal*, Vol. 53, No. 6, 2015, pp. 1627–1639. https://doi.org/10.2514/1.j053467.

[4] Arntz, A., "Civil aircraft aero-thermo-propulsive performance assessment by an exergy analysis of high-fidelity CFD-RANS Flow Solutions," Ph.D. thesis, Lille 1 University - Sciences and Technologies, 2014. URL https://hal.archives-ouvertes.fr/tel-01113135.

[5] Arntz, A., and Hue, D., "Exergy-Based Performance Assessment of the NASA Common Research Model," *AIAA Journal*, Vol. 54, No. 1, 2016, pp. 88–100. https://doi.org/10.2514/1.j054127.

[6] Arntz, A., and Atinault, O., "Exergy-Based Performance Assessment of a Blended Wing–Body with Boundary-Layer Ingestion," *AIAA Journal*, Vol. 53, No. 12, 2015, pp. 3766–3776. https://doi.org/10.2514/1.j054072.

[7] Wiart, L., and Negulescu, C., "Exploration of the Airbus Nautilius Engine Integration Concept," *31st Congress of the International Council of the Aeronautical Sciences (ICAS)*, 2018. URL http://www.icas.org/ICAS_ARCHIVE/ICAS2018/data/papers/ICAS2018_0135_paper.pdf.

[8] Couilleaux, A., and Arntz, A., "Exergy Analysis for a CFD-Based Turbofan Exhaust Mixer Performance Improvement," *3AF International Conference on Applied Aerodynamics*, 2018. 3AF Paper FP28-AERO2018.

[9] Petropoulos, I., and Sartor, F., "Aerodynamic performance analysis of an isolated UHBR engine using a far-field exergy balance method," *57th 3AF International Conference on Applied Aerodynamics*, 2023. URL https://hal.science/hal-04065787, 3AF Paper AERO2023-20.

[10] Petropoulos, I., Wervaecke, C., Bailly, D., and Derweduwen, T., "Numerical investigations of the exergy balance method for aerodynamic performance evaluation," *AIAA Aviation 2019 Forum*, American Institute of Aeronautics and Astronautics, 2019. https://doi.org/10.2514/6.2019-2926, AIAA Paper 2019-2926.

[11] Petropoulos, I., Bailly, D., and Berhouni, I., "Development of numerical accuracy indicators for the far-field exergy balance method," *AIAA Aviation Forum*, 2023. https://doi.org/10.2514/6.2023-3389, AIAA Paper 2023-3389.

[12] Aguirre, M. Á., and Duplaa, S., "Exergetic Drag Characteristic Curves," *AIAA Journal*, Vol. 57, No. 7, 2019, pp. 2746–2757. https://doi.org/10.2514/1.j057985.

[13] Aguirre, M. Á., Duplaa, S., Carbonneau, X., and Turnbull, A., "Velocity Decomposition Method for Exergy-Based Drag Prediction," *AIAA Journal*, Vol. 58, No. 11, 2020, pp. 4686–4701. https://doi.org/10.2514/1.j059414.

[14] Aguirre, M. Á., "Exergy analysis of innovative aircraft with aeropropulsive coupling," Ph.D. thesis, 2022. URL http://www.theses.fr/2022ESAE0008.

[15] Fiore, M., "Influence of cavity flow on turbine aerodynamics," Ph.D. thesis, ISAE-Institut Supérieur de l'Aéronautique et de l'Espace, 2019. URL http://www.theses.fr/2019ESAE0013.

[16] Berhouni, I., Bailly, D., and Petropoulos, I., "Exergy Balance Extension to Rotating Reference Frames: Application to a Propeller Configuration," *AIAA Journal*, Vol. 61, No. 4, 2023, pp. 1790–1806. https://doi.org/10.2514/1.J062216.

[17] Berhouni, I., Petropoulos, I., and Bailly, D., "Exergetic analysis of the NASA Rotor 37 compressor test case," *15th European Conference on Turbomachinery Fluid dynamics & Thermodynamics (ETC15)*, 2023. URL https://hal.science/hal-04099251, paper ETC2023-171.

[18] Ruscio, J., Duplaa, S., Aguirre, M. Á., and Binder, N., "Exergy Analysis of Unsteady Flow Around an Adiabatic Cylinder in Vortex Shedding Condition," *56th 3AF International Conference on Applied Aerodynamics*, 2022. 3AF Paper FP13-AERO2022.

[19] Ruscio, J. P., Duplaa, S., and Binder, N., "Unsteady exergy analysis of an airfoil (OAT15A) under transonic buffet condition," *57th 3AF International Conference on Applied Aerodynamics*, 2023. 3AF Paper AERO2023-83.

[20] Berhouni, I., Bailly, D., and Petropoulos, I., "On the adaptation of the exergy definition in the field of aerodynamics," *57th 3AF International Conference on Applied Aerodynamics*, 2023. URL https://hal.science/hal-04065846, 3AF Paper AERO2023-18.

[21] Drela, M., "Power Balance in Aerodynamic Flows," *AIAA Journal*, Vol. 47, No. 7, 2009, pp. 1761–1771. https://doi.org/10.2514/1.42409.

[22] Baskaran, P., Corte, B. D., van Sluis, M., and Rao, A. G., "Aeropropulsive Performance Analysis of Axisymmetric Fuselage Bodies for Boundary-Layer Ingestion Applications," *AIAA Journal*, Vol. 60, No. 3, 2022, pp. 1592–1611. https://doi.org/10.2514/1.j060362.

[23] Lamprakis, I., Sanders, D. S., and Laskaridis, P., "Energy-Based Aerodynamic Loss and Recovery Characteristics of Adiabatic and Heated Fuselages," *Journal of Aircraft*, 2023, pp. 1–19. https://doi.org/10.2514/1.c037246, Article in advance.

[24] Miller, R. J., "Mechanical Work Potential," *Proceedings of the ASME Turbo Expo 2013: Turbine Technical Conference and Exposition. Volume 6A: Turbomachinery*, American Society of Mechanical Engineers, 2013. https://doi.org/10.1115/gt2013-95488, Paper GT2013-95488.

[25] Jardine, L. J., and Miller, R. J., "The Effect of Heat Transfer on Turbine Performance," *Mechanical Engineering*, Vol. 142, No. 09, 2020, pp. 56–57. https://doi.org/10.1115/1.2020-sep5, Paper ME-2020-SEP5.

[26] Jardine, L., "The Effect of Heat Transfer on Turbine Performance," Ph.D. thesis, University of Cambridge, 2020. https://doi.org/10.17863/CAM.56517.

[27] Ruiz, J., "Jet Engines Performance Accounting," *25th ISABE Conference*, International Society for Air Breathing Engines, 2022. Paper ISABE-2021-093.